Gemi ve Deniz Teknolojisi Dergisi
Sayı: 225, Haziran 2024
ISSN: 1300-197, e-ISSN: 2651-530X, Dergi ana sayfası: http://www.gmoshipmar.org/
Araştırma Makalesi

Salınımlı Su Kolonu (OWC) için Güç Çıkışı ve Verimin Deneysel Olarak Doğrulanması

Şafak Nur Ertürk Bozkurtoğlu

Gemi İnşaatı ve Deniz Bilimleri Fakültesi, Gemi ve Deniz Teknolojisi Mühendisliği Bölümü, İstanbul Teknik Üniversitesi, Türkiye

erturk@itu.edu.tr, ORCID: 0000-0002-8494-1988

ÖZET

Küresel enerji talebinin artması ve fosil yakıtların çevresel etkilerine ilişkin endişeler nedeniyle daha temiz, sürdürülebilir alternatiflere acil ihtiyaç duyulmaktadır. Bu çalışma, yenilenebilir enerji bağlamında dalga enerjisinin kıyı yapılarının güç ihtiyaçlarına potansiyel katkısını vurgulamaktadır. Araştırma, kıyı yapılarına entegre edilebilecek, böylece bu yapıların güç ihtiyacının bir kısmını karşılayabilecek bir Salınımlı Su Kolonu (OWC) sistemi için güç çıkışı ve verimliliği değerlendirmektedir. Hem teorik hesaplamalardan hem de 1:10 ölçekli bir model deneyinden elde edilen bulgular sunulmuştur. Tam bir prototip için sistemin çıkış gücü ve verimliliği, 3 m dalga yüksekliğine sahip derin su koşulları için hesaplanmıştır. Hazne içindeki su yüzeyi salınımının hazne dışında meydana gelen salınımı yansıttığı varsayılmıştır. Tam ölçekli prototip için 22.5 m dalga boyuna karşılık gelen maksimum ortalama mekanik güç çıkışı 64.8 kW olarak belirlenmiş ve %64.4'lük bir mekanik verim elde edilmiştir. Sistemin genel verimliliği, jeneratör verimliliğinin %85 olduğu varsayılarak %55 olarak hesaplanmış ve bu da yaklaşık 55 kW'lık bir ortalama güç çıktısı sağlamıştır. Wells türbinli OWC sisteminin 1:10 ölçekli bir modeli oluşturulmuş ve derin su koşulları için bir tankta test edilmiştir. Froude benzerliği ve Keulegan-Carpenter benzerliği kullanılarak modelden prototipe sorunsuz bir geçiş sağlanmıştır. OWC modeli, T = 1.2 s periyotla kontrollü dalıp-çıkma hareketine tabi tutulmuştur. OWC modeli tarafından üretilen güç, Wells türbini üzerindeki entegre dört adet 3.4 V LED'i aydınlatmış ve bu da üretilen güç çıkışını ölçmek için kullanılmıştır. Modelin güç çıkışı 107 rpm dönüş hızı için minimum 0.12 W olarak ölçülmüştür ve bu da ölçeklendirilmiş prototip için 12 kW'lık bir güç çıkışına karşılık gelmektedir. Bu sistem, dalga etkisine maruz kalan kıyı yapılarına birden fazla OWC'nin dahil edilmesiyle daha fazla geliştirilme potansiyeline sahiptir. Bu tür bir gelişme, kıyı yapılarının güç gereksinimlerinin karşılanmasını kolaylaştırabilir ve böylece hem yenilenebilir enerji üretiminin hem de sürdürülebilir bir çevrenin teşvik edilmesine katkıda bulunabilir. Gelecekteki araştırmalar, belirli sahalar için OWC hazne boyutlarını optimize etme ve su yüzeyi salınım dinamiklerini daha iyi yakalayacak şekilde modeli iyileştirmeye odaklanacaktır.

Anahtar Kelimeler: Yenilenebilir enerji, dalga enerjisi, salınımlı su sütunu, sürdürülebilirlik

Makale geçmişi: Geliş 14/12/2023– Kabul 19/05/2024

https://10.54926/gdt.1405048

GMO Journal of Ship and Marine Technology
Issue: 225, June 2024
ISSN: 1300-1973, e-ISSN: 2651-530X, Journal homepage: http://www.gmoshipmar.org/
Research Article

Experimental Validation of Power Output and Efficiency for an Oscillating Water Column (OWC)

Şafak Nur Ertürk Bozkurtoğlu

Faculty of Naval Architecture and Ocean Engineering, Department of Shipbuilding and Ocean Engineering, İstanbul Technical University, Türkiye

erturk@itu.edu.tr, ORCID: 0000-0002-8494-1988

ABSTRACT

With the global energy demand escalating and concerns over the environmental impact of fossil fuels, there's a pressing need for cleaner, sustainable alternatives. This study highlights the potential contribution of wave energy to the power needs of coastal structures in the context of renewable energy. The research evaluates the power output and efficiency for an Oscillating Water Column (OWC) system that can be integrated into coastal structures to meet part of their power needs. Findings from both theoretical calculations and a 1:10 scale model experiment are presented. The mechanical power output and efficiency of the system for a full-scale prototype were calculated for deep water conditions with a wave height of 3m. The water surface oscillation inside the chamber is assumed to reflect the oscillation occurring outside the chamber. The maximum average mechanical power output for the full-scale prototype, corresponding to a wavelength of 22.5 m, was determined to be 64.8 kW, achieving a mechanical efficiency of 64.4 %. The overall efficiency of the system is calculated as 55 % by assuming the generator efficiency to be 85 %, resulting in an average power output of approximately 55 kW. A 1:10 scale model of the OWC system with a Wells turbine was constructed and tested in a tank for deep water conditions. Froude similarity and Keulegan-Carpenter similarity were used, ensuring a seamless transition from the model to the prototype. The OWC model was subjected to controlled heaving motion with a period of T = 1.2 s. The power generated by the OWC model illuminated four integrated 3.4 V LEDs on the Wells turbine, which were used to measure the power output produced. The power output of the model was measured to be a minimum of 0.12 W for a rotational speed of 107 rpm, which corresponds to a power output of 12 kW for the scaled-up prototype. This system has the potential for further enhancement by incorporating multiple OWCs into coastal structures exposed to wave action. Such development could facilitate meeting the power requirements of coastal structures, thereby contributing to the promotion of both renewable energy generation and a sustainable environment. Future research will focus on optimizing OWC chamber sizes for specific sites and refining the model to better capture water surface oscillation dynamics.

Keywords: Renewable energy, wave energy, oscillating water column, sustainability

Article history: Received 14/12/2023 – Accepted 19/05/2024

1. Introduction

While the world's energy needs are constantly increasing recently, much of it is met by fossil fuels. However, the harm that fossil fuels have on the environment is an important consideration. This issue relates to industrialized and developing countries that signed the Kyoto Protocol in 1997 to control and reduce carbon emissions in the atmosphere. The Kyoto Protocol was an amendment to the United Nations Framework Convention on Climate Change (UNFCCC), a pivotal international treaty that was entered into force on March 21, 1994, aimed at mitigating global warming (*Kyoto Protocol to the United Nations Framework Convention on Climate Change*, 2023). By uniting nations, its primary objective was to address the inevitable consequences of rising temperatures. The protocol imposed legally binding provisions on ratifying countries, surpassing the strength of those outlined in the UNFCCC. The Kyoto Protocol established precise emission reduction targets for industrialized countries, with an exemption for developing countries. In order to achieve these targets, most countries that ratified the protocol were required to employ various strategies. One prominent strategy involved a shift towards enhanced utilization of renewable energy sources, such as solar power, wind power, ocean energy, and biodiesel, as substitutes for conventional fossil fuels.

While the majority of industrialized nations endorsed the Kyoto Protocol, economic considerations led some signatory countries to express reservations (Shishlov et al., 2016). Despite being finalized in Kyoto, Japan, in 1997, the protocol only took effect in 2005 after extensive negotiations. As the 1997 Kyoto Protocol focused on developed countries, only 84 countries signed it and implemented the framework. But 196 countries have signed the 2015 Paris Agreement, which goes even further and places responsibility on all countries to limit emissions (*The Paris Agreement, UNFCCC*, 2024). Meanwhile, the severity of environmental pollution stemming from fossil fuels has escalated significantly. In addition to relying on fossil fuels, many developed countries constructed nuclear power plants to fulfill their energy requirements and derive energy from nuclear sources. However, the potential for natural disasters, substantial negligence, and other factors pose a significant risk. As a result, nations with nuclear power plants are progressively opting for the phased closure of these facilities as a strategy to mitigate the associated risks (*PRIS - Reactor Status Reports - Permanent Shutdown - By Country*, 2024).

Extensive research has been conducted in the realm of clean energy to mitigate the potential disasters stemming from the misuse of nuclear power plants and the pollution associated with fossil fuels. The outcomes of these investigations have fueled a growing inclination towards renewable energy sources (Dey et al., 2022). This shift is characterized by a heightened focus on energy alternatives that substantially decrease environmental pollution. As a result, the adoption of renewable energy is on the rise, reflecting a concerted effort to address environmental concerns and promote sustainable energy practices.

Given Türkiye's unique geographical positioning with three sides surrounded by seas, a strategic focus on wave energy sources is a necessity. Although the wave potential might not be ample for significant clean energy generation, it is important for newly constructed coastal structures to be designed to meet at least a portion of their energy requirements. Retrofitting existing coastal structures with wave energy converters, if possible, should also be considered. For such a goal, an Oscillating Water Column (OWC) system is one of the best alternatives (Zheng et al., 2019). The main focus of this study concerns the theoretical estimation of both the efficiency and potential power output generated by an OWC system specifically designed for integration into coastal structures. The aim is to support these

theoretical assessments with experimental findings and ultimately aim to meet the power requirements of coastal structures.

1.1. Wave energy converters

Ocean waves contain tremendous energy potential. When it comes to energy production from the oceans, energy production from the waves is the most advantageous commercial method and is preferred by many companies (Minerals Management Service, 2006). Wave energy exhibits a range of advantages and drawbacks. On the positive side, it is renewable, environmentally friendly, abundant, predictable, and poses no harm to land. Harnessing this energy is relatively straightforward. Conversely, it is limited to specific locations, can have adverse effects on marine ecosystems (Grecian et al., 2010; Hutchison et al., 2022), disrupts vessel traffic, introduces noise and visual pollution (Patricio et al., 2009), and underperforms in inclement weather conditions.

Wave Energy Converters (WECs) are devices designed to harness energy from either the movement of waves at the surface or the pressure variations beneath the water's surface. These devices generate electricity using one of the following three functions: wave motion, wave pressure, and air pressure. These systems are further divided into two as fixed or floating systems. The wave energy is obtained from the movement of the equipment which is fixed to the float or seabed. While numerous designs and concepts exist, WECs can generally be categorized into three main types: attenuators, point absorbers, and terminators (Drew et al., 2009). Attenuators are systems with floating parts that move with the waves. They use wave motion as the driving force. The kinetic energy of the wave moves the turbines and drives electricity generation. Pelamis® is an example of such systems (Rodrigues, 2008). Point absorbers make use of the pressure difference created by the rising and falling water level due to the wave action to generate electricity. These structures can either be floating, moving up and down on the water's surface, or submerged below the water surface (Drew et al., 2009). Terminators are positioned perpendicular to the wave direction. These devices typically include a component that moves up and down in response to the waves. This reciprocal motion is utilized to pressurize fluid, which in turn drives a turbine, generating energy. An example of a terminator-type WEC is the Salter's Duck, developed at the University of Edinburgh. (Falcão, 2010). It is also possible to classify WECs based on their operation modes. This classification includes submerged pressure differential devices, oscillating wave surge converters, oscillating water column (OWC) devices, and overtopping devices.

1.2. OWC Systems

OWC systems represent a first-generation of WECs and are widely used in coastline applications. One of the earliest OWC system was integrated into a cliff at Toftestallen, near Bergen in 1985. Another small OWC shoreline prototype was deployed at the island of Islay, Scotland in 1991 (Falcão, 2010; Henriques et al., 2016). UK, Portugal, India, and Japan are the leading countries that installed and are still working on OWC systems (Cruz, 2008). OWC systems are preferred more often by energy companies because of the cheaper and easier cost and maintenance compared to other WEC systems. OWC systems have the flexibility to be constructed onshore, nearshore, or offshore. Nevertheless, each location comes with its distinct set of drawbacks: offshore structures have disadvantages such as high maintenance costs and difficulties in energy transfer, while systems in the shallow zone should be durable to cope with the increased kinetic energy due to the breaking of waves approaching the shore. The deployment of shoreline devices could be limited by the shoreline geology, tidal range and the

requirements of preservation of coastal scenery, etc. (Cruz, 2008).

Conversely, a well-designed OWC system tailored to the specific site can generate sufficient power to fulfill the energy requirements of the structure it is integrated into. These systems, integrated into marine structures like ports, docks, etc. offer an alternative to high-carbon footprint generators. Their value becomes particularly evident as they generate electricity consistently, even in unfavorable weather conditions when the city's power grid may face challenges. Thus, they emerge as an ideal tool for environmental sustainability.

OWC systems (Figure 1) are typically designed to be stationary. The fundamental principle of OWC technology involves harnessing energy through the rotation of an air turbine driven by the movement of air trapped and released during wave oscillation. In these systems, seawater brought in by the waves enters through the bottom of an enclosed structure, known as the chamber. As the water rises within the chamber, it compresses the air inside. At the top of the OWC system, a turbine is placed. The compressed air is directed to the turbine through a specially designed funneling interior. Subsequently, as the gravity-driven wave recedes, it creates a vacuum within the system, leading to the influx of external air through the turbine. This airflow causes the turbine to rotate, thereby converting the wave energy into mechanical energy. By connecting a generator to the turbine, the mechanical energy generated can be further transformed into electrical energy. This process illustrates how OWC systems facilitate the conversion of wave energy into a usable and sustainable form of power.

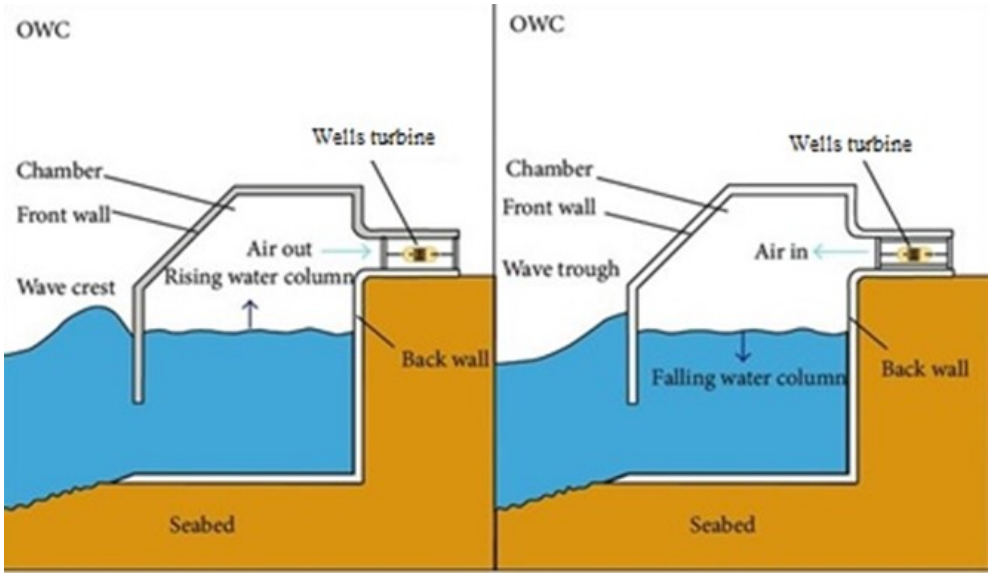

Figure 1. Schematic layout of an OWC system at compression and suction stages (Cui & Liu, 2015)

Conventional turbines are typically engineered for fluid movement in a specific direction. Consequently, when integrated into OWC energy conversion systems, these turbines may generate energy either during the compression of air or its suction, leading to a reduction in overall efficiency. To optimize energy production and capture the maximum potential of the system, a self-rectifying turbine becomes essential. This specialized turbine rotates consistently in the same direction during both the air compression and suction stages, ensuring enhanced efficiency throughout the OWC energy conversion process.

While OWC systems boast a straightforward structure, they offer significant prospects for development and efficiency enhancements. Extensive research has been conducted on OWC systems

(Brito-Melo et al., 2002; Josset & Clément, 2007; Martins-Rivas & Mei, 2009; Orphin et al., 2022). Despite the progress made, it's important to note that OWC systems are still undergoing development.

1.3. Wells Turbine

Presently, three types of self-rectifying air turbines are in use: Wells Turbine, Impulse Turbine and Dennis-Auld Turbine. Wells Turbines capable of bi-directional operation is best suited for the OWC systems. The Wells Turbine (Figure 2), was first conceptualized in 1980 in Belfast (Čarija et al., 2012). The most important feature of the Wells turbine is that each airfoil blade is symmetrical for the axis passing through the blade center.

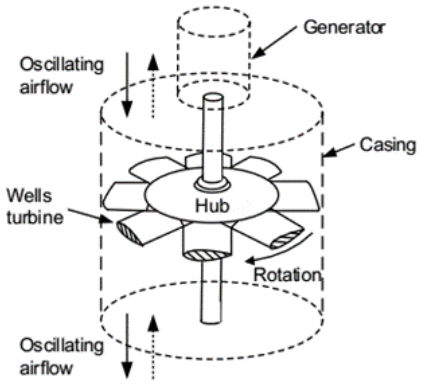

Figure 2. Outline of Wells' turbine (Okuhara et al., 2013)

Symmetric airfoil blades, positioned around an axis of rotation, rotate in the tangential force direction which acts only in one direction independent of the direction of airflow (Mohamed, 2011) (Figure 3). Consequently, the Wells turbine exhibits a stable rotation in one direction, ensuring continuous power generation for the connected electrical generator, irrespective of changes in the airflow direction. If the airfoil is oriented at an angle of attack α within a fluid flow, it generates a lift force *L*, perpendicular to the free stream, and a drag force, *D*, aligned with the direction of the free stream. The combined aerodynamic force, F_R, resulting from the lift and drag forces, is expressed as follows:

$$F_R = \sqrt{L^2 + D^2} \tag{1}$$

The resultant force can be decomposed into its axial and tangential components, F_A and F_t respectively. These components can be further expressed in terms of lift and drag as:

$$F_A = Lcos\alpha + Dsin\alpha \tag{2}$$

$$F_t = Lsin\alpha - Dcos\alpha \tag{3}$$

The tangential force, denoted as F_t, is accountable for generating torque, thereby contributing to the blade power. On the other hand, the axial force, represented as F_A, leads to an axial thrust along the rotor's axis. In the context of a symmetrical airfoil section, the tangential force F_t retains its direction for both positive and negative values of α, whereas the axial force F_A undergoes a reversal in its direction. This results in a unidirectional rotation of the device when exposed to alternating airflow (Mohamed, 2011).

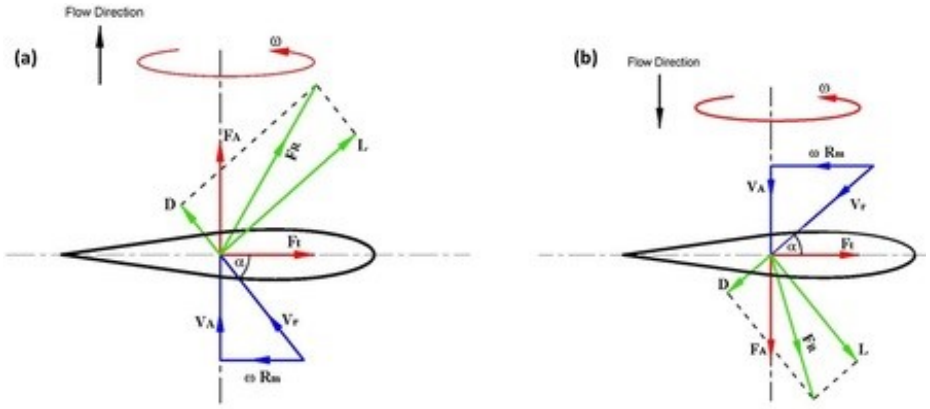

Figure 3. Aerodynamic forces acting on a Wells turbine blade (a) compression stage, (b) suction stage (Shehata et al., 2017)

2. Materials and Methods

Coastal structures, such as breakwaters, offshore platforms, and submerged pipelines, may encounter deep water conditions depending on their location and the characteristics of the surrounding ocean or sea. These conditions are crucial considerations in the design and assessment of coastal structures to ensure their stability, functionality, and resilience against wave action and other environmental forces. A 1:10 scale oscillating water column (OWC) model was constructed for experimental evaluation. Theoretical computations were conducted to ascertain its performance under deep water conditions.

The choice of model scale and the depth of the testing tank were pivotal in establishing the upper limit of the oscillation period. The lower limit of the period was determined based on the critical wave steepness value that could lead to wave breaking. Subsequently, calculations were performed to determine various parameters including wave length, wave power, rotational power, and system efficiency. The OWC model underwent controlled heaving motion within the tank, where the minimum power output was gauged through the illumination of LEDs. The resultant power data from the OWC model experiment was then scaled up and compared with the theoretical estimations for the prototype. These steps are explained in detail in the following subheadings.

2.1 Model Construction

The aim of this research is to design an OWC system for integration into marine structures, particularly breakwaters. The objective is to provide a sustainable energy solution for these structures, inherently exposed to wave loading. In this context, a model of an OWC system suitable for integration with marine structures has been constructed. The emphasis is on the simplicity of the working principle and the ease of installation at a laboratory scale. OWCs are designed to produce electrical energy by converting wave energy. These systems have equipment that provides the electrical cycle as well as chambers where the increasing water column compresses the air inside. In the OWC operating principle, the turbine takes its energy from the compressed air stream, although the energy is harnessed from the wave.

The OWC system in this study comprises two main components: a chamber for compressing and pressurizing air and a Wells turbine utilizing the air pressure difference as the driving force to generate electricity. The subsequent subheadings provide a detailed description of the Wells turbine

construction and chamber design for the 1:10 scale model.

2.1.1. Construction of Wells Turbine

A 20 cm diameter LED (Light Emitting Diot) computer fan (Figure 4a) was employed as a substitute for the Wells turbine, generator, and rotor assembly (Figure 2). Due to the incompatibility of the computer fan blades with those of a Wells turbine, they were removed (Figure 4b) and are set to be replaced with blades that align with the Wells turbine design.

Figure 4.a) 20 cm DC12V 0.30A LED computer fan b) The skeleton of the fan with the original blades removed

Typically designed for electricity consumption, computer fans operate as consumers of electrical power. In adapting the existing computer fan for use as a Wells turbine, a crucial transformation was required: shifting the fan's role from an electricity consumer to an electricity generator. This necessitated a modification of the fan's original circuitry to facilitate the generation of electricity. Initially, the modification process involved the removal of the Integrated Circuit (IC) pin. Figure 5a shows four slender copper wire windings and the detached IC pin.

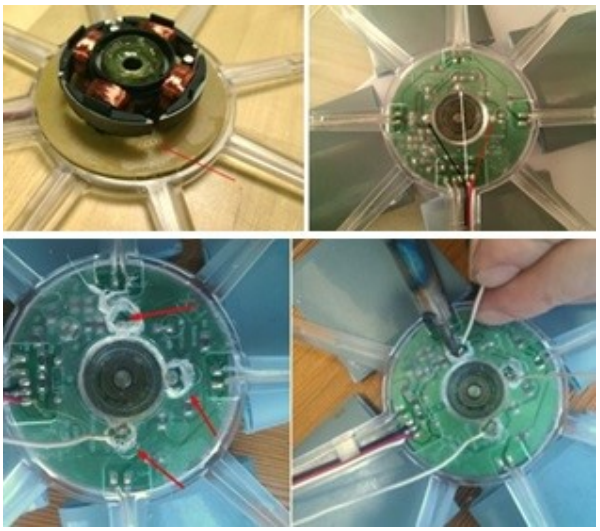

Figure 5. a) Copper wire windings and detached IC pin, b) Connection points of copper wires at the back of the fan, c) Drilling holes in the cover section, d) Soldering copper cables to copper windings.

The red and black copper wires on the fan (Figure 5b) serve to regulate the incoming current circuit, while the white copper wire is employed for adjusting the rotational speed. The copper wire windings are soldered to the points indicated by the arrows in Figure 5b. There are magnets inside the main body where the blades are mounted and the rotor is connected. When the rotation takes place, electric

current is generated on the copper wire windings. To facilitate the transfer of the generated electricity, holes were drilled in the cover section (Figure 5c). Subsequently, copper cables were soldered (Figure 5d) to copper windings, establishing a connection for the transmission of the generated electricity to the targeted circuit.

To optimize the aerodynamic performance of the turbine model, the original blades were replaced with new ones designed to conform to the NACA0020 airfoil profile. The NACA0020 airfoil profile, well-known for its high efficiency, is widely recognized as one of the predominant blade profiles utilized in Wells turbines (Cruz, 2008), (Shehata et al., 2017). Six symmetrical blades were constructed and affixed to the fan body. A quarter circle with an outer radius of 9 cm and an inner radius of 3 cm was cut from PVC, Styrofoam was inserted inside, folded symmetrically, and the edges were joined (Figure 6) to form the new blades.

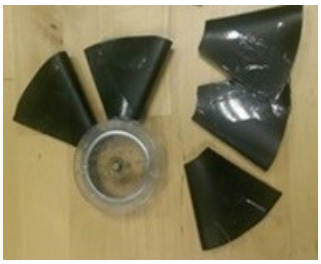

Figure 6. Side view of the six symmetrical sectioned NACA0020 blades

2.1.2. Construction of the Chamber

The next step in this study was to design a chamber in which the elevated water would compress the air and the compressed air would rotate the blades of the Wells turbine. A simple OWC chamber model is constructed with a truncated cone-shaped plastic container. The model chamber has an outlet diameter of 30 cm and an inlet diameter of 40 cm. The construction of the OWC model was completed by mounting the Wells turbine with a fan diameter of 20 cm at the outlet of the chamber model. A schematic representation of the OWC system along with the solid model is given in Figure 7.

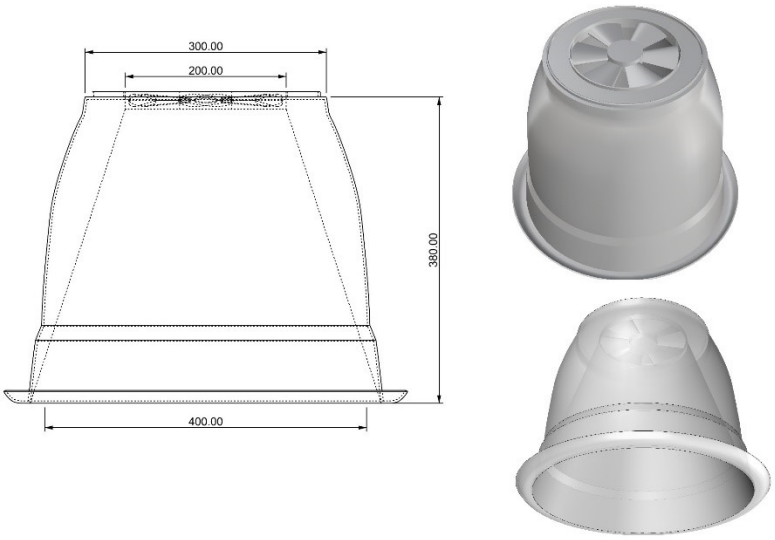

Figure 7. Geometric properties and the solid model of the OWC system.

The inner surface of the chamber is covered with a plastic layer to ensure a conical geometry. This configuration accelerates the flow inside the chamber and efficiently directs the air flow to the turbine. In addition, a layer of silicone is applied between the plastic sheet and the chamber to ensure a secure seal.

2.2. Calculation of Wave Power (P_w)

The wave power (P_w) and the wavelength (λ) are determined using the standard linear wave theory (Heller, 2012) for deep and shallow water conditions, as follows:

$$P_{w,deep} = \rho_{water} g^2 T H^2 w / 32\pi \,, \qquad \lambda = gT^2/2\pi \tag{4}$$

$$P_{w,shallow} = \rho_{water} g^2 T H^2 \mathrm{dw} / 8\lambda \,, \qquad \lambda = \frac{gT^2}{2\pi} tanhkd \tag{5}$$

where ρ_{water} is the water density, g is the gravitational acceleration, T is the wave period, d is the water depth, w is the width of the wave crest presented to the chamber, H is the wave height and k is the wave number, which is:

$$k = 2\pi/\lambda \tag{6}$$

2.3. Calculation of Mechanical Power Output (P_t)

A schematic representation of a forcing linear wave profile and the corresponding wave properties is provided in Figure 8, along with the depiction of the OWC system utilized in this study. In the employed model, the water-air chamber is in the form of a truncated cone, with circular inlet and outlet sections. The methodology for calculating the power output of the OWC system relies on the heave velocity of the water column within the chamber, derived from the displacement value.

The volumetric air-flow rate into the OWC chamber can be calculated as:

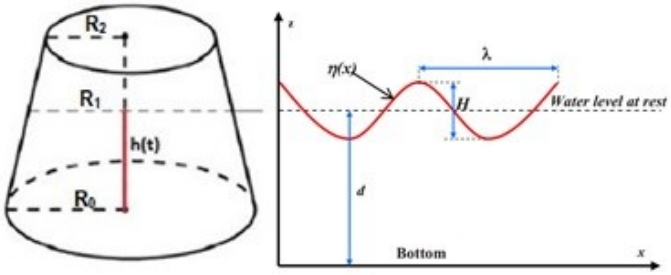

Figure 8. The model chamber and water wave properties. R_1 is the radius of the model chamber at the still water level (SWL), R_0 is the inlet radius, R_2 is the outlet radius of the chamber model and h(t) is the water level time series inside the chamber. λ is the wavelength, H is the wave height, d is the water depth.

$$Q = A_1 V_1 \tag{7}$$

where A_1 is the cross-sectional area of the water column at the SWL in the chamber and V_1 is the

average velocity of the water column at the SWL in the chamber (Kelly et al., 2013).

Using the continuity equation, the average output velocity V_2 can be calculated.

$$V_2 = \frac{A_1 V_1}{A_2} = \frac{\pi R_1^2 V_1}{\pi R_2^2} = \left(\frac{R_1}{R_2}\right)^2 V_1 \tag{8}$$

If we assume that the maximum water level change in the chamber will be $h_{max} = H$ in time $T/2$ then the average air velocity at the SWL, V_1 will be

$$V_1 = \frac{h_{max}}{T/2} \tag{9}$$

Combining Equation (8) and Equation (9), the average air velocity at the outlet, V_2, is found

$$V_2 = \left(\frac{R_1}{R_2}\right)^2 \frac{2H}{T} \tag{10}$$

The airflow velocity at the blades, namely V_2, is directly proportional to the wave height and decreases as the wave period increases.

The water level change in the chamber can be expressed as:

$$\eta(x,t) = \frac{H}{2}\, sin(kx - \sigma t) \tag{11}$$

The initial volume of air confined in the chamber at the initial time t_0 is

$$\forall_c = \frac{\pi m}{3}[R_1^3 - R_2^3] \tag{12}$$

where m is the slope of the lateral surface of the chamber.

The volume of sucked/compressed air, $\forall_w(t)$, at time t as a result of change in water level is:

$$\forall_w(t) = \frac{\pi m}{3}\left[R_1^3 - \left(R_1 - \frac{H}{2m} sin(kx - \sigma t)\right)^3\right] \tag{13}$$

The volume of air trapped in the chamber at time t is the initial volume of air plus/minus the sucked/compressed air volume which is:

$$\forall_{air}(t) = \forall_c - \forall_w(t) \tag{14}$$

$$\forall_{air}(t) = \frac{\pi m}{3}\left[\left(R_1 - \frac{H}{2m}\sin(kx - \sigma t)\right)^3 - R_2^3\right] \tag{15}$$

$$\dot{m}_{in} - \dot{m}_{out} = \frac{dm_{cv}}{dt} \tag{16}$$

The rate of change of the air volume $\dot{\forall}_{air}(t)$ is the air volume flow rate passing through the turbine

$$\dot{\forall}_{air}(t) = \frac{d\forall_{air}(t)}{dt} = \pi\sigma\left[\left(R_1 - \frac{H}{2m}sin(kx - \sigma t)\right)^2\right]\left[\frac{H}{2}cos(kx - \sigma t)\right] \quad (17)$$

A wind turbine captures kinetic energy from the airflow, characterized by the speed V_{air} and mass flow rate $\dot{m}_{air}$ and transforms it into mechanical rotational power. Applying the Bertz's limit (16/27) (University of South Florida & Blackwood, 2016) which is the theoretical maximum efficiency for a wind turbine, we can write the total mechanical rotational power of the system as:

$$P_t = \frac{1}{2}\left(\frac{16}{27}\right)\dot{m}_{air}V_{air}^2 = \frac{8}{27}\frac{\rho_{air}}{A_c^2}\dot{\forall}_{air}(t)^3 \quad (18)$$

where ρ_{air} is the air density and A_c is the turbine cross-section area. The total delivered energy during one period T of the incident wave can be expressed as:

$$E_t = 4\int_0^{T/4} P_t dt \quad (19)$$

The mechanical efficiency (%) of the system in converting wave power to rotational power is given by:

$$\eta_P = (P_t/P_w) \times 100 \quad (20)$$

where P_t is the average rotational power output of the system, P_w is the mean wave power transmitted for width w of the wave front in the direction of wave propagation.

2.4 Experimental Setup

The model is tested in a tank at the Ata Nutku Ship Model Testing Laboratory located at ITU Faculty of Naval Architecture and Ocean Engineering. The tank width is 1.4 m and the water depth is 1.3 m. The schematic depiction of both the model OWC system and the tank's geometric configuration is illustrated in Figure 9.

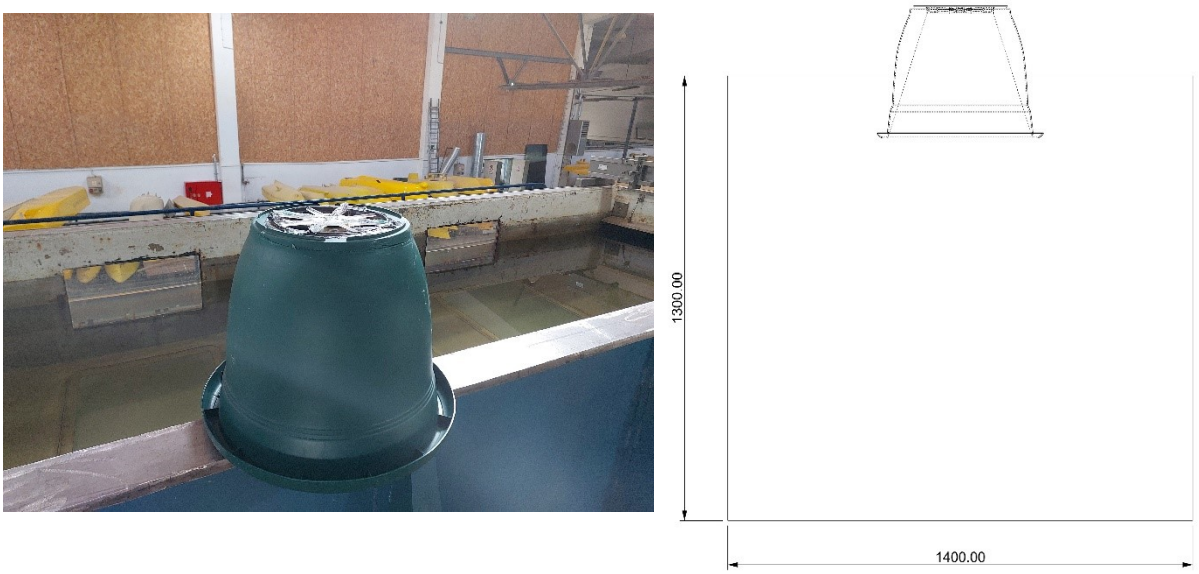

Figure 9. The OWC model and schematic layout of the model and the tank geometry.

The circuit on the electronic board of the computer fan has four 3.4 V LEDs. Initially, the electric circuit of the model is tested by blowing air to force the blades to rotate. The rotation of the blades induced rotation in the rotor, generating an electrical current along the copper wires, consequently lighting up the LEDs. The OWC system model is then tested in the tank to see whether the water elevation inside the chamber is sufficient to trigger rotation of the blades. The rotation of the blades is effectively driven by the airflow generated through the water level changes within the chamber. A voltmeter is used for measuring the potential difference (V) across the circuit integrated on the electronic board of the Wells turbine. During the model experiments, while the wave forcing was manually generated, recordings were captured using a high frame rate camera, and the applied wave period was determined through analysis of these recordings.

3. Results and Discussion

3.1. Experimental Results for the Model

The OWC model was forced manually to heave in the tank with a period of $T = 1.2\ s$. This period value is within the range of deep-water condition. Remarkably, the power generated by the simple model OWC system proved sufficient to illuminate all four 3.4 V LEDs (Figure 10). The LED serves as an indicator, emitting light only when it receives sufficient electrical power, making it a useful tool for measuring the power generated by the model OWC.

Figure 10. Four 3.4 V blue LEDs are illuminated.

A voltmeter recorded a 2 V potential difference across the circuit integrated on the electronic board of the Wells turbine in the tank, when LEDs emit low brightness light. The forward current and brightness of LEDs vary depending on both the semiconductor material and applied voltage. The terminal voltage was changed by using a variable voltage source, and the total system current at the terminals that is summation of the currents of all system elements such as LEDs, coils, driver etc. was measured. The change of total system current with terminal voltage of the fan is given in Table 1.

Table 1. The change of total current with terminal voltage of the fan

Terminal Voltage (V_{DC})	Total system current (mA)	LED brightness
2.6	32	low brightness
4	60	normal brightness
6	103	normal brightness
8	146	high brightness
10	190	high brightness

It was seen from the experiments that the model is capable to generate electrical power. Since the air turbines within OWCs operate at low rotational speeds, it's crucial to identify the ideal turbine rotational speed and develop an energy-optimized control system (Rosati et al., 2022). Measurements, including rotational speed, voltage, current, and frequency, were also performed. As a sample case, at a rotational speed of 107 rpm, the voltage was measured as 6 V, the current drawn by a single LED was 5 mA. Under this operating condition, the total led current is calculated as $I = 4 \times 0.005\ A = 0.02\ A$, the consumed power on 4 LEDs is calculated as $P_{consumed} = 6\ V \times 0.02\ A = 0.12\ Watts$. Considering the model scale, the prototype power output is expected to be 10^5 times the model power output, leading to a power output of 12 kW for the scaled-up prototype.

Since the fan motor used in the model is a brushless motor, it generates AC electrical power, and both the frequency and terminal voltage depend on rotational speed. When assessing the model's feasibility for a specific location, choosing the right electrical generator is crucial. According to literature (Amilibia & Iturregi, 2010), two generator types suitable for use with variable-speed turbines in wave-based power generation are the synchronous permanent magnet generator (PMG) with the frequency inverter and the asynchronous induction generator. The efficiencies of PMGs and DFIGs (Double Fed Induction Generators) range from 0.86 to 0.95 depending on the type and size of the generator.

3.2. Theoretical Results for the Prototype

The geometric properties of the model and prototype OWC are given in Table 2. Froude (Fr) similarity and Keulegan-Carpenter (KC) similarity are used respectively, for scaling up the model heave velocity and model period to full-scale prototype values. Thus, the prototype period is found to be √10 times the model period (T_m = 1.2 s), which corresponds to T = 3.8 s for the prototype.

Table 2. Model and prototype OWC parameters.

Parameter	Model	Prototype
Inlet Diameter [m]	0.40	4.0
Outlet Diameter [m]	0.20	2.0
Diameter at SWL [m]	0.15	1.5
Chamber Height [m]	0.38	3.8
Wave Height [m]	0.30	3.0
Period [s]	1.20	3.8
Deep water wave length [m]	2.25	22.5

Equation 4 was employed to calculate the wave power (P_w), Equation 18 was used for the mechanical power output (P_t), and Equation 20 was used for determining the mechanical efficiency (η_p) values corresponding to various wavelengths. The outcomes of these calculations are presented in Table 3.

At the determined wave height, rotational power and mechanical efficiency increase as the wave length decreases. Deep water waves break when the wave steepness H/λ reaches the threshold value of (1/7) (Dean and Dalrymple , 1994). In our case, for a 3 m wave height the lower limit for the wavelength is $\lambda = 21\ m$. This is the lowest wavelength that a deep-water wave with the specified height can maintain its stability. Below this value, the wave will break. On the other hand, when the wavelength exceeds $\lambda = 26\ m$, deep water condition is violated. This is the upper limit for the wavelength. The scaled-up wavelength for the prototype, $\lambda = 22.5\ m$, falls within this range.

Table 3. Variations of mechanical power output and efficiency versus wavelength for the prototype

Prototype	Deep Water Condition			Intermediate Water Condition										
T [s]	3.67	3.80	4.00	4.38	4.73	5.00	5.37	5.66	5.93	6.20	6.45	6.70	6.93	7.16
λ_o [m]	21	22.5	25	30	35	40	45	50	55	60	65	70	75	80
λ [m]	21	22.5	25	29.9	34.4	38.8	43.1	46.9	50.7	54.4	57.8	61.2	64.1	67.1
P_t [kW]	71.9	64.8	55.5	42.3	33.6	28.4	22.9	19.6	17.0	14.9	13.2	11.8	10.6	9.7
η_P [%]	73.9	64.4	52.4	36.4	26.8	21.4	16.1	13.0	10.8	9.1	7.8	6.7	5.8	5.1

The maximum instantaneous air volume flow rate (Figure 11a), maximum instantaneous mechanical power output and average mechanical power (Figure 11b) were calculated for the scaled-up prototype, where the period is T = 3.8 s. The average mechanical power output for the prototype was determined to be 64.8 kW with a mechanical efficiency of η_p = 64.4 % (Table 3).

The rate of airflow through the turbine fluctuates over time in response to variations in the water level within the tapered chamber (Figure 11a). The volume flow rate is taken as positive during the suction stage where air in the chamber flows in the downward direction. The volume flow rate is taken as negative during the compression stage where the air in the chamber flows in the upward direction. The volume flow rate is zero at the end of the suction and compression stages where the air motion halts and changes direction. The first 0.95 seconds of one period is the suction stage where the water level keeps going down. The compression stage takes place between 0.95 and 2.85 seconds of one period and the water level goes up in this stage. The mechanical power output of the system varies over time (Figure 11b**)**, reaching zero at the 0.95 and 2.85 seconds, corresponding to instances of zero flowrate. Suction takes place again between 2.85 and 3.8 seconds.

The average mechanical power output for the full-scale prototype, corresponding to a wavelength of 22.5 m, was determined to be 64.8 kW, achieving a mechanical efficiency of 64.4 %. The overall efficiency of a system can be calculated by multiplying efficiencies of all equipment such as turbine, electrical generator, connection elements etc. The overall efficiency of the proposed system can be calculated as 55 % by taking generator's efficiency as 85 % in which case the average power output of the system will be around 55 kW. The losses in other components may reduce the overall efficiency. The resulting efficiency value is promising and not less than the range applicable to most air turbines. Air turbines typically operate at an efficiency range of 20 % to 40 % in converting wind into energy (“Renewable Energy Fact Sheet: Wind Turbines,” 2013).

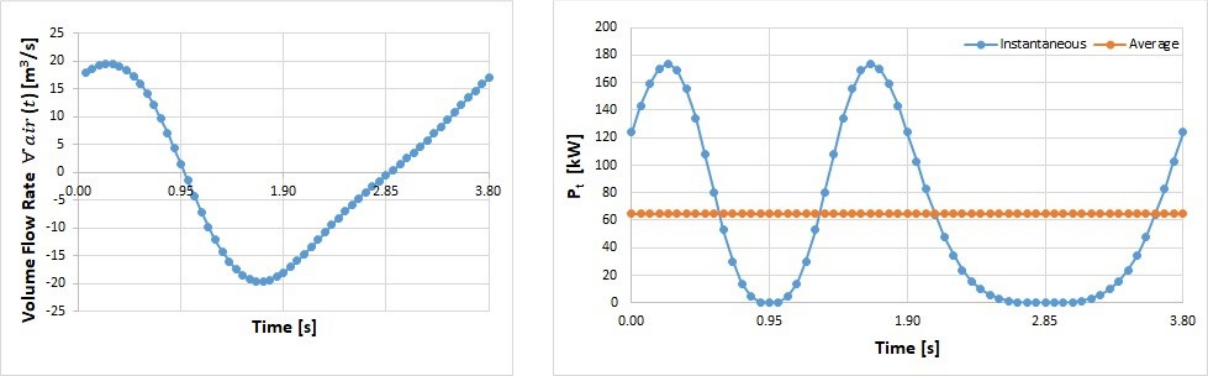

Figure 11. a) Maximum instantaneous air volume flow rate, b) Maximum instantaneous mechanical power output and average mechanical power.

The main objective of the numerical calculation pertaining to the efficiency of OWC systems is to model the oscillations of the free surface within the reservoir. The findings presented in this context may not offer an exact representation of the flow dynamics within the chamber. The assumption is that the oscillation of the water surface inside the chamber mirrors that of the oscillation outside the chamber. However, the fluctuation of the water free-surface inside the chamber, influenced by actual sea conditions, will introduce a level of uncertainty.

4. Conclusion

It is feasible to provide at least a portion of the energy needed by coastal structures through wave energy within the scope of clean energy. In this study, the power output and efficiency of an OWC system that could be considered in the design of new coastal structures or integrated into existing coastal structures through retrofitting have been calculated, and the results have been compared with the findings of a 1:10 scale model experiment. The study reveals that the mechanical power output is directly proportional to the cube of the wave height (H) and inversely proportional to the cross-sectional area of the air inlet/outlet (A_c). Notably, the relationship between the mechanical power output and the wave length is nonlinear (Table 3). Both the mechanical power output and mechanical efficiency exhibit a decrease as the wavelength increases. Intriguingly, the maximum values for both the mechanical power output and mechanical efficiency coincide at the same wavelength.

OWC systems should be designed and installed considering parameters such as the regional wave climate, the wave length, wave period and water depth. In the conducted study, an illustrative case was resolved under deep-water conditions, assuming a wave height (H) of 3 m. The results indicate that the maximum power achieved was 64.8 kW with an accompanying mechanical efficiency of 64.4 %. The optimal performance occurred at a specific wave length (λ) of 22.5 m.

In a particular region, the most frequently observed wavelength and wave height can be employed to ascertain the optimal dimensions of an OWC chamber, aiming for maximum mechanical power output and efficiency. Future research will involve a parametric study aimed at optimizing the dimensions of an OWC chamber for a selected site and will focus on developing a more accurate model for water surface oscillation within the chamber.

Acknowledgements

The author would like to acknowledge the resources and support of ITU Faculty of Naval Architecture and Ocean Engineering Ata Nutku Ship Model Testing Laboratory. The author would also like to express gratitude to Prof. Dr. Mustafa Bağrıyanık for his invaluable feedback on the electrical calculation sections of this article.

References

Amilibia, J. L., & Iturregi, A. (2010). Selection of the Electrical Generator for a Wave Energy Converter.Renewable Energy and Power Quality Journal, 1, 125–134. https://doi.org/10.24084/repqj08.255

Brito-Melo, A., Gato, L. M. C., & Sarmento, A. J. N. A. (2002). Analysis of Wells turbine design parameters by numerical simulation of the OWC performance. *Ocean Engineering*, *29*(12), 1463–1477. https://doi.org/10.1016/S0029-8018(01)00099-3

Čarija, Z., Kranjčević, L., Banić, V., & Čavrak, M. (2012). Numerical analysis of wells turbine for wave power conversion. *Engineering Review*, *32*(3), 141–146.

Cruz, J. (2008). Ocean Wave Energy Current Status and Future Prepectives. In *Springer Series in Green Energy and Technology*. https://doi.org/10.2174/97816080528511060101

Cui, Y., & Liu, Z. (2015). Effects of Solidity Ratio on Performance of OWC Impulse Turbine. *Advances in Mechanical Engineering*, *7*(1), 1–10. https://doi.org/10.1155/2014/121373

Dean R.G., & Dalrymple R.A. (1994). *Water Wave Mechanics for Engineers and Scientists*. World Scientific Publishing.

Dey, S., Sreenivasulu, A., Veerendra, G. T. N., Rao, K. V., & Babu, P. S. S. A. (2022). Renewable energy present status and future potentials in India: An overview. *Innovation and Green Development*, *1*(1), 100006. https://doi.org/10.1016/j.igd.2022.100006

Drew, B., Plummer, A. R., & Sahinkaya, M. N. (2009). A review of wave energy converter technology. *Proceedings of the Institution of Mechanical Engineers, Part A: Journal of Power and Energy*, *223*(8), 887–902. https://doi.org/10.1243/09576509JPE782

Falcão, A. F. de O. (2010). Wave energy utilization: A review of the technologies. *Renewable and Sustainable Energy Reviews*, *14*(3), 899–918. https://doi.org/10.1016/j.rser.2009.11.003

Grecian, W., INGER, R., Attrill, M., Bearhop, S., Godley, B., Witt, M., & Votier, S. (2010). Potential impacts of wave-powered marine renewable energy installations on marine birds. *Ibis*, *152*, 683–697. https://doi.org/10.1111/j.1474-919X.2010.01048.x

Heller, V. (2012). Development of Wave Devices from Initial Conception to Commercial Demonstration. In *Comprehensive Renewable Energy* (pp. 79–110). Elsevier. https://doi.org/10.1016/B978-0-08-087872-0.00804-0

Henriques, J. C. C., Portillo, J. C. C., Gato, L. M. C., Gomes, R. P. F., Ferreira, D. N., & Falcão, A. F. O. (2016). Design of oscillating-water-column wave energy converters with an application to self-powered sensor buoys. *Energy*, *112*, 852–867. https://doi.org/10.1016/j.energy.2016.06.054

Hutchison, Z. L., Lieber, L., Miller, R. G., & Williamson, B. J. (2022). Environmental Impacts of Tidal and Wave Energy Converters. In *Comprehensive Renewable Energy* (pp. 258–290). Elsevier. https://doi.org/10.1016/B978-0-12-819727-1.00115-1

Josset, C., & Clément, A. H. (2007). A time-domain numerical simulator for oscillating water column wave power plants. *Renewable Energy*, *32*(8), 1379–1402. https://doi.org/10.1016/j.renene.2006.04.016

Kelly, T., Dooley, T., Campbell, J., & Ringwood, J. V. (2013). Comparison of the experimental and numerical results of modelling a 32-oscillatingwater column (OWC), V-shaped floating wave energy converter. *Energies*, *6*(8), 4045–4077. https://doi.org/10.3390/en6084045

Kyoto Protocol to the United Nations Framework Convention on Climate Change. (2023). Audiovisual Library of International Law. https://legal.un.org/avl/ha/kpccc/kpccc.html

Martins-Rivas, H., & Mei, C. C. (2009). Wave power extraction from an oscillating water column at the tip of a breakwater. *Journal of Fluid Mechanics*, *626*, 395–414. https://doi.org/10.1017/S0022112009005990

Minerals Management Service. (2006). Wave Energy Potential on the U.S. Outer Continental Shelf Introduction. *Renewable Energy and Alternate Use Program*, *May*. http://ocsenergy.anl.gov

Mohamed, M. H. A. (2011). Design Optimization of Savonius and Wells Turbines [Otto-von-Guericke-Universit at Magdeburg]. In *Faculty of Process and Systems Engineering: Vol. Doktoringe*. https://www.mendeley.com/catalogue/design-optimization-savonius-wells-turbines/

Okuhara, S., Takao, M., Takami, A., & Setoguchi, T. (2013). Wells Turbine for Wave Energy Conversion—Improvement of the Performance by Means of Impulse Turbine for Bi-Directional Flow. *Open Journal of Fluid Dynamics*, *03*(02), 36–41. https://doi.org/10.4236/ojfd.2013.32A006

Orphin, J., Nader, J.-R., & Penesis, I. (2022). Size matters: Scale effects of an OWC wave energy converter. *Renewable Energy*, *185*, 111–122. https://doi.org/10.1016/j.renene.2021.11.121

Patricio, S., Moura, A., & Simas, T. (2009). Wave energy and underwater noise: State of art and uncertainties. In *OCEANS '09 IEEE Bremen: Balancing Technology with Future Needs* (p. 5). https://doi.org/10.1109/OCEANSE.2009.5278302

PRIS - Reactor status reports—Permanent Shutdown—By Country. (2024, February 11). https://pris.iaea.org/PRIS/WorldStatistics/ShutdownReactorsByCountry.aspx

Renewable Energy Fact Sheet: Wind Turbines. (2013). *United States Environmental Protection Agency*.

Rodrigues, L. (2008). Wave power conversion systems for electrical energy production. *Renewable Energy and Power Quality Journal*, *1*(06), 601–607. https://doi.org/10.24084/repqj06.380

Rosati, M., Henriques, J. C. C., & Ringwood, J. V. (2022). Oscillating-water-column wave energy converters: A critical review of numerical modelling and control. *Energy Conversion and Management: X*, *16*, 100322. https://doi.org/10.1016/j.ecmx.2022.100322

Shehata, A. S., Xiao, Q., Saqr, K. M., & Alexander, D. (2017). Wells turbine for wave energy conversion: A review. *International Journal of Energy Research*. https://doi.org/10.1002/er.3583

Shishlov, I., Morel, R., & Bellassen, V. (2016). Compliance of the Parties to the Kyoto Protocol in the first commitment period. *Climate Policy*, *16*(6), 768–782. https://doi.org/10.1080/14693062.2016.1164658

The Paris Agreement, UNFCCC. (2024, February 9). https://unfccc.int/process-and-meetings/the-paris-agreement

University of South Florida, & Blackwood, M. (2016). Maximum Efficiency of a Wind Turbine. *Undergraduate Journal of Mathematical Modeling: One + Two*, *6*(2). https://doi.org/10.5038/2326-3652.6.2.4865

Zheng, S., Zhang, Y., & Iglesias, G. (2019). Coast/breakwater-integrated OWC: A theoretical model. *Marine Structures*, *66*, 121–135. https://doi.org/10.1016/j.marstruc.2019.04.001